STEADY STATE 3-D SIMULATION OF CANDU6 MODERATOR CIRCULATION UNDER THE NORMAL OPERATING CONDITION

Churl Yoon, Bo Wook Rhee, Byung-Joo Min

Korea Atomic Energy Research Institute
150 Dukjin-Dong, Yusong-Gu, Daejeon 305-353, Korea
Phone: +82-42-868-2986, Fax: +82-42-868-8590, E-mail: bwrhee@kaeri.re.kr

ABSTRACT

Moderator circulation inside the CANDU-6 reactor vessel of Wolsong 2/3/4 (KOREA) under normal operating condition is analyzed by using computational fluid dynamics for predicting the local subcooling of the moderator in the vicinity of the calandria tubes. The buoyancy effect induced by internal heating is accounted for by the Boussinesq approximation. The standard k-ε turbulence model associated with logarithmic wall treatment is applied to predict the turbulent jet flows from eight inlet nozzles. The matrix of calandria tubes in the core region is simplified as porous media, in which anisotropic hydraulic impedance is modeled using an empirical correlation of frictional pressure loss. The governing equations are solved by CFX-4.4, a commercial CFD code developed by AEA technology. The CFD model has been successfully validated against experimental data obtained in the Stern Laboratories Inc. (SLI) in Hamilton, Ontario. Steady-state 3-D prediction of the CANDU-6 moderator circulation under normal operating conditions gives a maximum moderator temperature of 82.9^{o}C at the upper core region, which corresponds to the minimum subcooling temperature of 24.8^{o}C considering hydro-static pressure increase. The flow pattern on the normal plane to z-axis is determined as ‘mixed-type’.

1. INTRODUCTION

The main roles of CANDU D_2O moderator are to moderate fast neutrons into thermal neutrons, to remove the heat generated during the moderation, and to act as the ultimate heat sink for some loss of coolant accidents with coincident loss of emergency core cooling, etc. For some loss of coolant accidents with coincident loss of emergency core cooling in a CANDU reactor, fuel channel integrity depends on the capability of the moderator to act as the ultimate heat sink. Predicting temperature distributions of moderator inside the calandria vessel under nominal operating conditions and LOCA transients are critical issues in the CANDU safety analysis. However, the computer codes that predict moderator temperatures for these accidents have not been adequately validated, given the small safety margins that exist currently. The objectives of this study are to develop a CFD model for predicting CANDU-6 moderator temperatures, to validate the model against available experimental data, and to predict steady-state velocity field and temperature distribution of Wolsong 2/3/4 moderator under normal operating conditions.

Figure 1 illustrates CANDU-6 moderator system. The calandria vessel is an indented cylinder 6.0 m long with a main-shell diameter of 7.60 m and a sub-shell diameter of 6.76 m. Each of the sub-shells has a length of 0.97 m. In addition to 380 calandria tubes inside the vessel, there are a number of horizontal and vertical reactivity mechanisms, which are omitted in this figure and analysis. The moderator fluid is heavy water at about atmospheric cover pressure. The moderator fluid is extracted from the vessel through two outlet ports located at the bottom of the vessel. The two outlet ports are symmetrically located with respect to the mid-plane perpendicular to the z-axis, but are asymmetrically placed at a cross-sectional view from a channel fixed end. After discharging through the outlet ports, the fluid mixes in a header, passes through one of two operating pumps to be cooled via parallel heat exchangers and is returned to the calandria through eight inlet nozzles located at the side of the vessel. The inlet nozzles are symmetrically placed in the x-y plane with respect to the vertical centerline but are asymmetrically placed in axial direction.

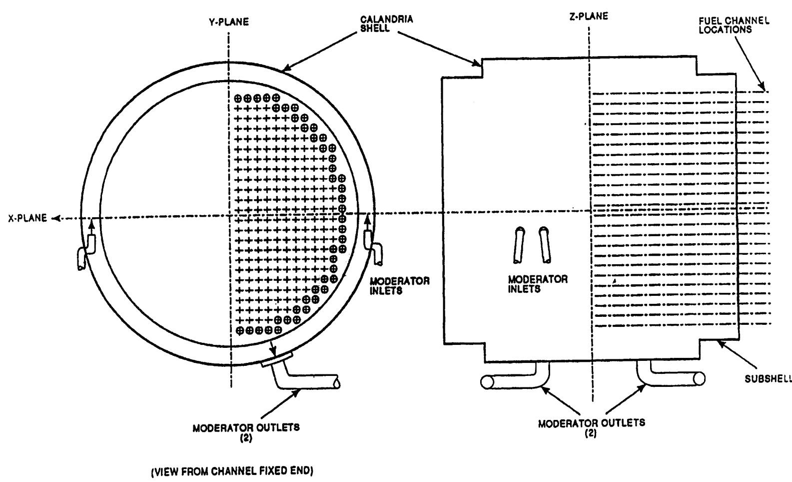

Figure 1: CANDU-6 Moderator System

Carlucci and Cheung [1] investigated the two-dimensional flow of internally heated fluid in a circular vessel to study the flow patterns inside a calandria vessel. There was a matrix of heating pipes at the center region of the circular vessel, which has two inlet nozzles at the sides and outlets at the bottom of the vessel. It was observed that the flow pattern inside the circular vessel were determined depending on the ratio of characteristic buoyancy to inertia forces, the non-dimensional Archimedes number (Ar), for the given geometry. Two distinct types of flow patterns are observed, jet-momentum-dominated for low Ar and buoyancy-dominated for high Ar. There was transition range of Ar number that represented a 'mixed-type' flow pattern between jet-momentum-dominated and buoyancy-dominated flow patterns. It was also observed that the resultant steady-state flow pattern could be oscillating between buoyancy-dominant flow and momentum-dominated flow periodically in the condition of a certain range of the Archimedes number.

In 1995, Collins [2] performed a moderator circulation analysis under normal operating conditions for Wolsong 2, 3, & 4 using the PHOENICS2 computer code. It was concluded that a steady-state solution could not be achieved and that only quasi-steady solutions could be achieved. It was also reported that a fully converged steady state solution had been obtained when the inlet velocity had been increased by a factor of 1.5(~3.0 m/s). In this quasi-steady solution, the maximum temperature within the moderator over the period 0~300 s varies between its lowest value of 78.5 ^{o}C and the highest of 81.7 ^{o}C.

In 1995, Seodijono et al. [3] performed transient moderator analyses after a large reactor inlet header break with failure of ECC injection. It was concluded that subcooling remains above 26 ^{o}C when Class IV power is available. When Class IV power is not available, the temperature of the top portion of the moderator inside the calandria vessel increases continuously during the post-blowdown phase to reach the saturation temperature.

2. MODEL DEVELOPMENT

For the thermal hydraulic analysis of the CANDU-6 moderator, the general purpose CFD code, CFX-4.4(AEA Technology), is used to solve a continuity equation, momentum equations and a energy equation coincidently. The finite-volume method is used. The advection terms are discretized by a first-order accurate Hybrid differencing scheme, while centred differencing schemes are used for other terms. The flow is assumed to be steady, incompressible and single-phase. The SIMPLEC algorithm is used, which is recommended for the flow with strong Buoyancy effect. The Boussinesq approximation is applied to model buoyancy forces, in which density in the momentum source term is a linear function of temperature and is constant in other terms of governing equations. The standard k-ε turbulence model associated with logarithmic wall treatment is used, as the flow field is known to be turbulent. CFX-4.4 uses the body-fitted grid with the Rhie-Chow interpolation rather than the staggered grid to simulate effectively the three-dimensional fluid flow in complex geometries.

The matrix of calandria tubes in the core region is simplified by the porous media approach [4]. The hydraulic resistance experienced by fluid flowing through the core region is accounted for as source terms of momentum equations. In the simulation of CANDU-6 moderator circulation and the prediction of local minimum subcooling of the moderator under normal operating conditions and LOCA transients, the resultant velocity fields and temperature predictions are very sensitive to the hydraulic resistance correlations for the porous region which represents a matrix of Calandria tubes.

HYDRAULIC RESISTANCE FOR POROUS MEDIA

The hydraulic resistance consists of two terms; the form drag term and the friction drag term. Neglecting the fact that hydraulic resistance is dependent on the attack angle between the flow direction and tube axis, the moderator fluid flow could be decomposed into axial flow and lateral flow conveniently.

For axial flow, there is no form drag. Thus, once when we assume that we can decompose fluid flow into x, y, and z components, the hydraulic resistance of axial flow could be expressed by the conventional correlations of frictional pressure loss in a cylindrical pipe.

$$\left.\frac{\Delta P}{\Delta L}\right)_z = \frac{\Delta P_{fric}}{\Delta z} = \frac{f\rho\, u_z^2}{2D_e} \tag{1}$$

Friction factor, f , is calculated from the friction factor correlation for the flow inside circular pipes. For the turbulent flow of a low Reynolds number,

$$f = 0.316 \cdot \mathrm{Re}^{-0.25} \tag{2}$$

Here, Reynolds number Re is defined by $u_z D_e / \nu$.

For the transverse(lateral) flow across the tube bank, Hadaller et al. [5] investigated the pressure drop of fluid flows crossing staggered and in-line tube banks, in which the Reynolds number range is 2,000 to 9,000 and pitch to tube diameter ratio is 2.16. Also, they concluded that for the given p/D ratio, the effect of staggering is not significant. From the results of Hadaller et al. [5], the obtained empirical correlation for the pressure loss coefficient is expressed as

$$\mathrm{PLC} \equiv \frac{\Delta \mathrm{P}}{\mathrm{N_r} \cdot \rho \cdot \frac{\mathrm{V_m}^2}{2}} = 4.54 * \mathrm{Re}^{-0.172}, \tag{3}$$

The hydraulic resistance source term in momentum equations are in a form of pressure drop per unit length.

$$\frac{\Delta P}{\Delta L} = \frac{N_r}{\Delta L} 4.54 \cdot \mathrm{Re}^{-0.172} \cdot \rho \cdot \frac{V_m^2}{2} \tag{4}$$

Here, $N_r / \Delta L$ can be expressed as an inverse of the pitch of the tube bank and the Reynolds number is defined as $V_m D / \nu$. Note that V_m is the velocity before entering the tube bank and that V_m is different from the local moderator velocity in the core region of CANDU calandria vessel, V_c.

$$V_m = \gamma_A V_c \tag{5}$$

Decomposition of pressure gradient per unit travel length gives

$$\left(\frac{\Delta P}{\Delta L}\right)_x = \frac{\Delta P}{\Delta L} \cos\theta = \frac{\Delta P}{\Delta L} \cdot \frac{u_x}{V_c} \tag{6}$$

$$\left(\frac{\Delta P}{\Delta L}\right)_y = \frac{\Delta P}{\Delta L} \cos\phi = \frac{\Delta P}{\Delta L} \cdot \frac{u_y}{V_c} \tag{7}$$

with θ is the angle between the fluid velocity vector and x-axis and ϕ is the angle between the fluid velocity vector and y-axis.

Now, Eq. (4) can be implemented as forms of the bellows.

$$\left.\frac{\Delta P}{\Delta L}\right)_i = \frac{1}{p} 4.54 \cdot \left(\frac{\gamma_A V_c D}{\nu}\right)^{-0.172} \cdot \rho \cdot \frac{\left(\gamma_A{}^2 V_c\right)}{2} u_i \tag{8}$$

The subscript i denotes x or y component.

Eq. (1) and eq. (8) are inserted into the momentum equations for the core region as source terms, to represent the hydraulic resistance of the tube bank matrix.

3. VALIDATION AGAINST EXPERIMENTAL DATA

Huget et al. [6,7] investigated experimentally the moderator circulation and temperature distribution of CANDU moderator under normal operating conditions and other conditions, using 2-dimensional moderator circulation facility at Stern Laboratories. They also provided the predicted velocity fields and temperature for each test case, using MODTURC_CLAS (MODerator TURbulent Circulation Co-Located Advanced Solution).

Figure 2 is a cross-sectional view of the test vessel in the Stern Laboratories Inc.(SLI) [6,7] The moderator test vessel is a cylinder with a diameter of 2 m and a length of 0.2 m. The vessel does not have scaled geometry from actual CANDU reactors and is rather close to a thin axial slice of a CANDU reactor. The working fluid is light water (H_2O). In the core region, there is a matrix of 440 heating pipes, which have an outer diameter of 0.033 m with a lattice pitch of 0.071 m. The width of the nozzle slot is variable from 8 mm to 16 mm and located at the horizontal centerline. The inlet nozzles span the full thickness (0.2 m) of the test vessel.

Measuring techniques used in these experiments are Laser Doppler Anemometry (LDA) for velocity measurements, T/C for temperature measurements, and a tracer technique using a PH indicator for flow visualization. Velocity measurements using LDA are obtained only for an isothermal test. The experimental data used for validation in this study are classified in the following three tests:

- an isothermal test with the nominal flow rate of 2.4 kg/s and no heat load
- the nominal-conditions test with a flow rate of 2.4 kg/s and a heat load of 100 kW
- a low-flow test with a flow rate of about 2 kg/s and the nominal heat load of 100 kW

The inlet temperature are maintained 55^{o}C for the nominal-conditions test and the low-flow test.

The assumptions and approximations developed for CANDU-6 moderator temperature prediction are used for the SLI simulation. A set of multi-block structured grids are generated and YPLUS values at the wall adjacent cell centroids are in the range of 10 ~ 150.

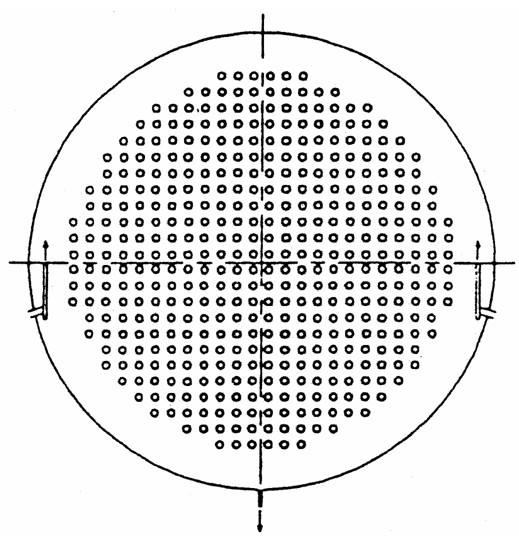

Figure 2: Test Section of Stern Lab. Experiments

<u>ISOTHERMAL TEST</u>

Figure 3 illustrates velocity field calculated by using CFX-4 for the isothermal test. Two inlet jets moves up the wall and collided at the top of the test vessel, forming a stagnation point. Figure 3 shows the velocity field of isothermal condition on the center plane perpendicular to the z-axis, simulated by CFX-4. The injected fluids from the two inlet nozzles moves up to the top and collides to make the stagnation point where the top wall and vertical centerline meet together. The flow pattern consisted of two large, roughly equal, counter-rotating vortices with centers located close to the edge of the core and at angles of about 35^o from vertical, which is well agreed with the experimental observation. The symmetry of the velocity field is well maintained

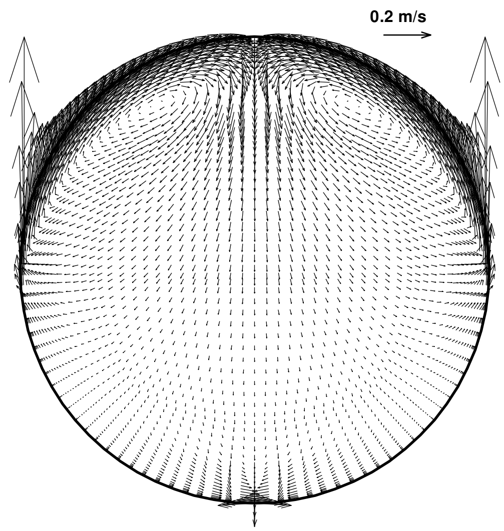

Figure 3: Velocity Field of Isothermal Condition, Simulated by CFX-4

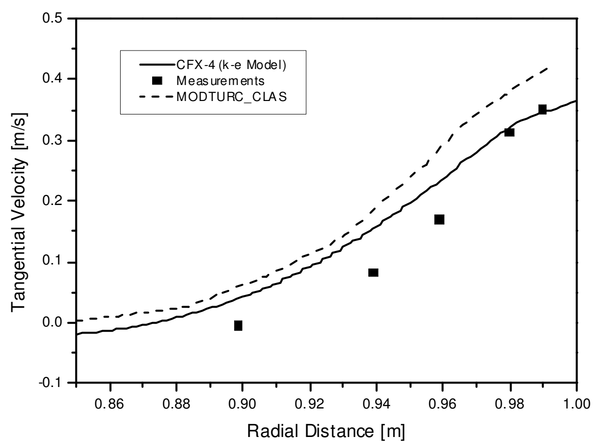

Figure 4: Tangential Velocity Profiles 30^o from Horizontal of Isothermal Condition

In Fig. 4 to Fig. 6, the velocity components are compared with LDA velocity measurements, at the vertical centerline in the tube bank and at two radial locations (30^o and 60^o from horizontal) in the jet development region. Kriging interpolation procedure [8] is adapted to calculate the velocity components at the required locations. Figure 4 and Figure 5 show the tangential velocity profiles in the reflector region of the vessel along radial lines displaced 30^o and 60^o respectively from the horizontal. Both the CFX-4 prediction and the former MODTURC_CLAS prediction are compared to LDA measurements. In Fig. 4 & 5, the current simulation using CFX-4 gives closer tangential velocity to the measurements. In Figure 4, the negative tangential velocities of the reflector region are observed near the core region, which is caused by the existence of large re-circulation flows.

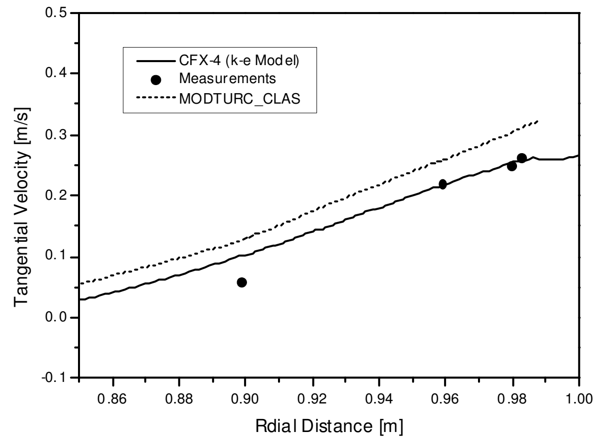

Figure 5: Tangential Velocity Profiles 60^{o} from Horizontal of Isothermal Condition

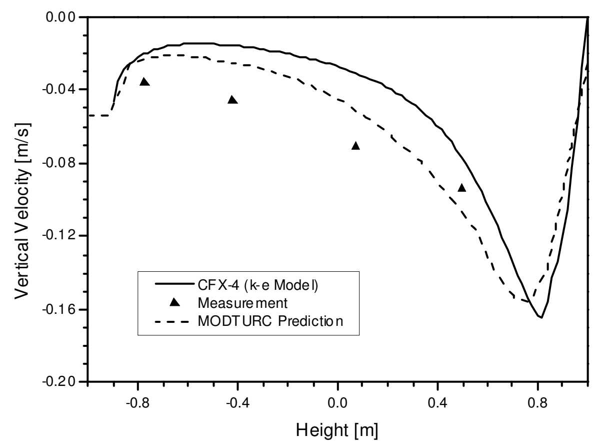

Figure 6: Vertical Velocities at the Vertical Centerline of Isothermal Condition

Figure 6 illustrates the vertical velocity profiles at the vertical centerline, with comparison to the experimental measurements and previous MODTURC_CLAS simulation results. The predictions of both codes are in good agreement with the experimental data. This comparison indicates that the empirical tube drag model for the core region in both CFX-4 and MODTURC_CLAS codes under-predicts velocity magnitudes in the core. The lower velocities in the core region generally would result in higher maximum temperatures when heat is generated, which is conservative from a subcooling viewpoint.

<u>NOMINAL-CONDITIONS TEST</u>

Total flow rate is 2.4 kg/s, the corresponding inlet velocity is 1 m/s, and the inlet temperatures are 55°C. The predicted velocity field and temperature distribution by using CFX-4 is not presented in this paper and can be found in a pervious work of the authors [9]. The flow pattern of nominal-condition test is found to be 'mixed-type'. In the results of the nominal-condition simulation, the flow reversal is observed only in one side. The cold injected fluid from the other side inlet nozzle goes all the way through the upper reflector region, guided by the upper circumferential vessel wall. The two injected fluids meet together at the angle of about 25° over the horizontal centerline, where the jet reversal occurs. The reversed fluid goes down to the bottom, guided by the circumferential lower vessel wall. The velocity vectors in most of the core region are sluggish and skewed upward. The temperature distribution shows a steep change of temperature around the jet reversal area. In this area, the fluid from the other side nozzle heated during the travel suppresses the cold injected fluid. The hottest spot is located at the upper center area of the core region, which slightly tilts to one side from the vertical centerline. The maximum temperature calculated by CFX-4 is about 73°C, close to the measured maximum temperature of 72.4°C.

The comparison of temperatures at the vertical centerline (X = 0 m) in the nominal-condition test is made in Fig. 7. The measured temperature and the predicted temperatures by MODTURC_CLAS computation using 35X21 grid and 51X25 grid are compared with the current simulation result. Figure 8 shows the temperatures at a horizontal line (Y=0.57 m) in the nominal-condition test. The predictions agree well with the measurements in the upper core region, but not quite well in the central core region.

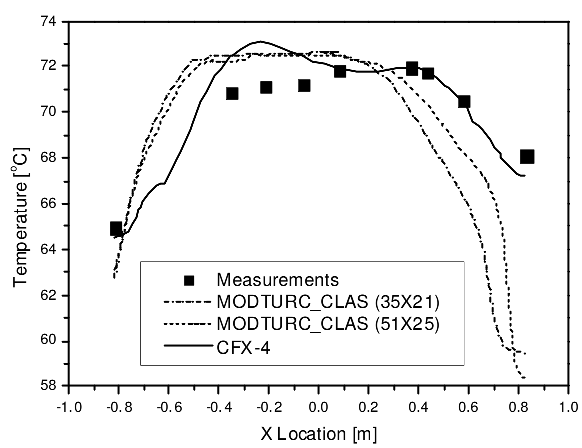

Figure 7: Temperatures at the Vertical Centerline in the Nominal-Condition Test

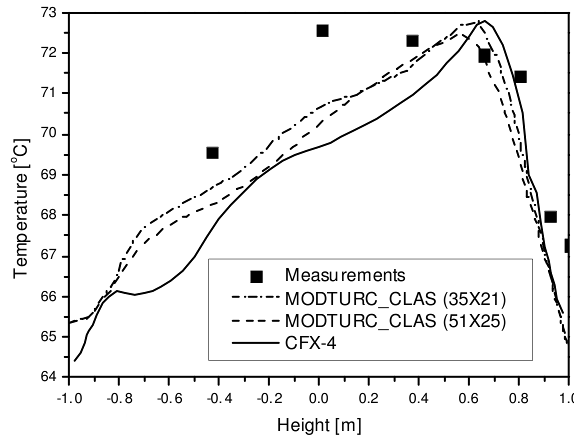

Figure 8: Temperatures at a Horizontal Line (Y=0.57 m) in the Nominal-Condition Test

LOW-FLOW TEST

The flow pattern for low-flow test is buoyancy-dominated. The cold injected fluid through the inlet nozzles changes its direction downward due to the suppression of hot fluid from the top of the test vessel. The reversed fluid goes down to the bottom, guided by the circumferential lower vessel wall. Most of these cold fluids at the bottom go out through the outlet, while some go up into the vacancy that is created by the elevation of heated fluid inside the porous region. Inside the central porous region, the elevation speed of hot fluid induced by buoyancy forces is relatively slow because of the hydraulic resistance.

4. MODERATOR CIRCULATION OF WOLSONG 2/3/4

Service water to the heat exchangers is controlled via the Moderator Temperature Control (MTC) program to maintain the calandria moderator outlet temperature at 69.0 °C. Under nominal full power conditions, the corresponding inlet temperature is approximately 45.0 °C. The inlet coolant velocity is of the order of 2 m/s at the nozzle entrance. The total flow rate through the eight nozzles is 940 L/s. Under normal operating conditions, nuclear heat generation induces 96.7 MW of power to the moderator fluid. In this study, the total heat load to the moderator is conservatively set 103 MW.

In the CANDU-6 moderator, heat is mostly generated by neutron and gamma direct heating and partially transferred from calandria tubes and other neighboring materials. Approximately 94% of the total heat load to the moderator is generated in the core region and the remaining 6% is generated in the reflector region. The local volumetric heat generation inside the moderator is spatially dependent on the power distribution of the core. Therefore, it is assumed that the function of volumetric heat generation of moderator is fractionally the same as the function of power distribution in the core region. For simplicity, it is assumed that the volumetric heat generation of moderator in the reflector region is uniform.

To implement the spatial power distribution, some typical power distribution inside the core region and the reflector region of Wolsong 2/3/4 have been chosen from their analysis reports. Based on the selected data, polynomial fittings have been performed in each axial and radial direction. Using the fitting formulas, the subroutine to implement the heat load distribution to the moderator has been made. Figure 9 shows the time-averaged axial power distribution for the M11 channel and its fitting equation. Figure 10 shows the time-averaged radial power distribution data and their fitting equation. From the power map, it is found that the trends in all radial outward directions are almost the same (symmetric). Thus, only one fitting equation is found and is angle-independent. R is the distance [m] from the center axis on the cross-sectional plane normal to z-axis. The fitting equations in fig. 9 and 10 are implemented into the energy equation as a heat source term.

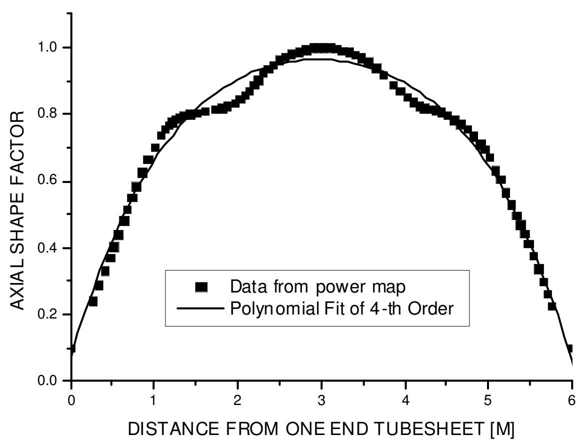

Figure 9: Time-Averaged Axial Power per Unit Volume of M11 and Channel and 4-th Order Polynomial Fit

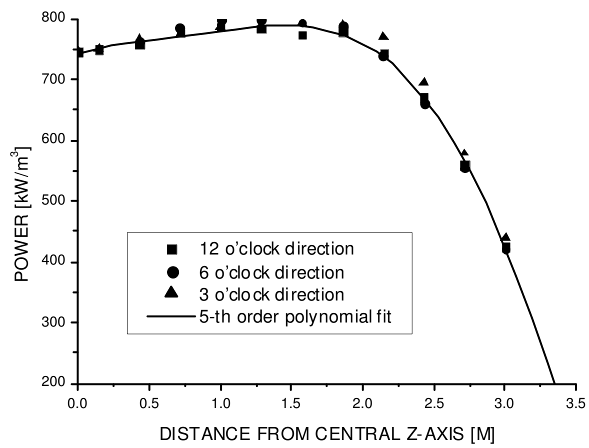

Figure 10: Time-Averaged Radial Power Distribution and 5-th Order Polynomial Fit

This steady state computation using CFX-4.4 was performed in an HP-C3600 workstation. The convergence criteria were the enthalpy residual reduction factor of 10^{-3} and the largest mass residual of 10^{-7}. Because the energy equation and momentum equations are strongly interrelated in this computation, the algebraic multi-grid solver and false time stepping technique were adapted to accelerate converging speed for the energy equation. The number of steady computation iterations was about 200,000~300,000.

The resultant velocity field and temperature distribution is presented in 3 slices of constant z and 1 slice of constant x. The z values of constant-z-slices were selected carefully. Therefore, two x-y planes include inlet nozzles and an outlet (Fig. 11 & 13), and the other constant-z slice contains neither nozzle nor outlet (Fig. 12), which represents the x-y plane between the inlets. The x value of constant-x-slice is 0.3 m (Fig. 14).

Figure 11 is the x-y plane z = 1.418 m away from one end tubesheet, where two inlet nozzles and an outlet are cut through. In Fig. 11(a), the flow reversal is observed only for the injected fluid from the inlet nozzle far from the outlet port. The cold injected fluid from the other side inlet nozzle goes all the way through the upper reflector region, guided by the upper circumferential vessel wall. The two injected fluids meet together at the angle of about 50^o over the horizontal centerline, where the jet reversal occurs. The reversed fluid goes down to the bottom, guided by the circumferential lower vessel wall. This asymmetry of flow pattern is induced by the interaction between the buoyancy forces and the inlet jet momentum forces. The velocity vectors in the core region are relatively small compared to those of the reflector region due to the hydraulic resistance in the core region. In Fig. 11(b), the temperature distribution shows a steep change of temperature around the jet reversal area. In this area, the fluid from the other side nozzle heated during the travel suppresses the cold injected fluid. The hottest spot is located at the upper center area of the core region, which slightly tilts to one side from the vertical centerline.

Figure 12 shows the velocity vectors and temperature contours in the cross section of z = 3.0 m away from the one end tubesheet. In this plane, neither the inlet nozzles nor the outlet appears. In Fig. 12(a), the flow pattern of the reflector region is similar to Fig. 11(a), except that there is neither inlet jet nor exiting velocity vector. The jet reversal does not appear. In Fig. 12(b), the hottest spot is located at the upper center area of the core region, which tilts to one side from the vertical centerline.

Figure 13 represents the velocity field and temperature distribution in the x-y plane of z = 4.582 m away from the one end tubesheet, where two inlet nozzles and an outlet appear. In Fig. 13(b), the hottest spot is located at the upper center area of the core region and the maximum temperature is 82.9^{o}C.

Figure 14 shows the velocity vectors and temperature distribution in the y-z plane that is 0.3 m away from the axis of the cylindrical calandria tank. From Fig. 14(a), it is shown that there is relatively small fluid movement in the z-direction around the center region. Note that the vector length is clearly increased to present relatively smaller velocity vectors. Near the outlets at the bottom of the main-shell, fluids go toward the closer outlet with relatively large speeds. In Figure 14(b), the isotherms at the lower part of the vessel indicate that the fluids in these areas are stratified. Note that the positions of the inlet nozzles are not symmetric across the central x-y plane (z = 3.0 m).

5. CONCLUSIONS & FUTURE WORKS

In this study, the CANDU moderator analysis model using CFX-4.4 is established and the simulation for predicting local subcooling of the moderator in the vicinity of calandria tubes in the CANDU6 reactor is performed. The temperature distributions and velocity fields of the simulation results are presented. With 103% full power for conservatism, the maximum temperature of the moderator is 82.9 ^{o}C at the top of the core region. Considering hydro-static pressure change, the minimum subcooling is 24.8 ^{o}C.

From the steady-state results by CFX-4 CFD simulation, the transient analyses for LOCA(Loss of Coolant Accidents) with loss of ECC(Emergency Core Cooling) injection will be performed for the future study.

ACKNOWLEDGMENTS

This study has been carried out as a part of the Development of Safety Issue Relevant Assessment System and Technology for CANDU NPPs program supported by Korea Ministry of Science & Technology.

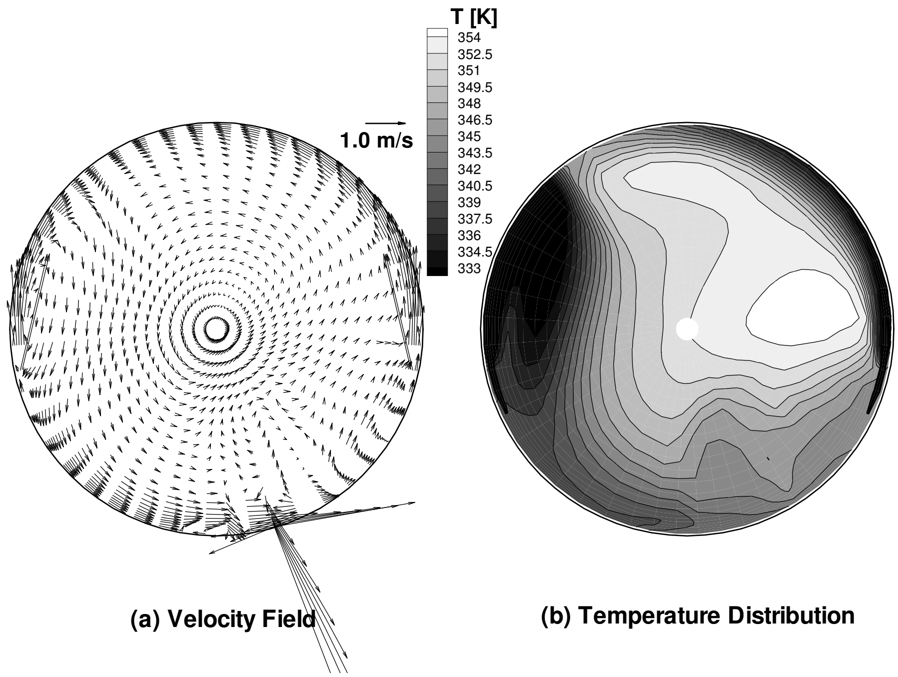

Figure 11: Steady-State Simulation Results for Wolsong 2/3/4 Moderator Using CFX-4; Cross-sectional View at 1.418 Meters Away from One End Tubesheet

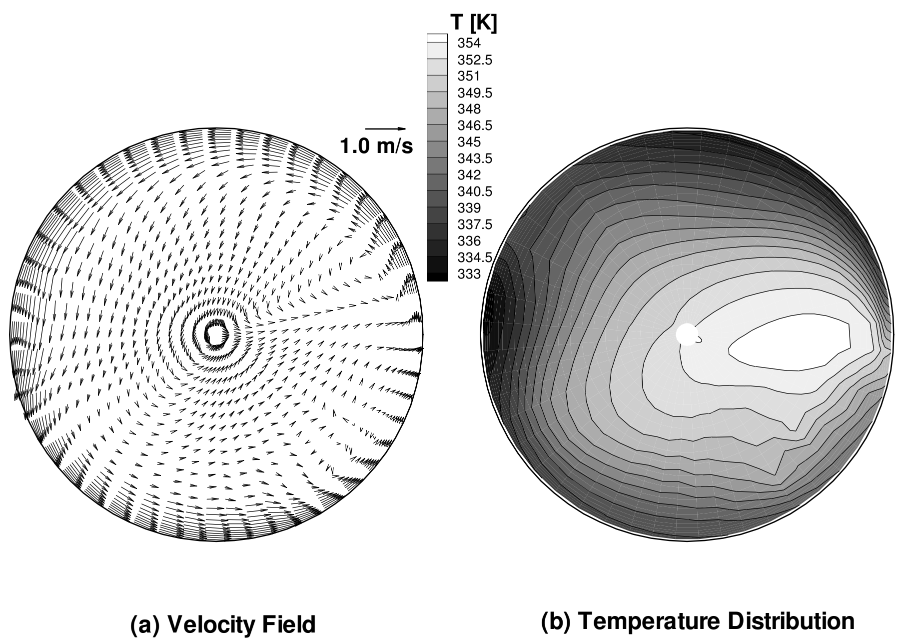

Figure 12: Steady-State Simulation Results for Wolsong 2/3/4 Moderator Using CFX-4; Cross-sectional View at 3.0 Meters Away from One End Tubesheet

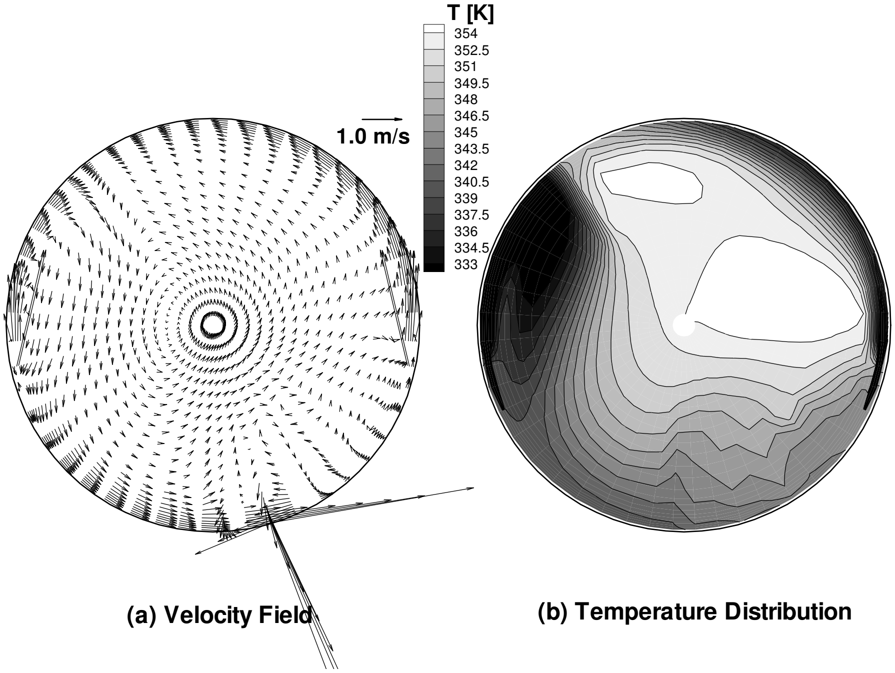

Figure 13: Steady-State Simulation Results for Wolsong 2/3/4 Moderator Using CFX-4; Cross-sectional View at 4.582 Meters Away from One End Tubesheet

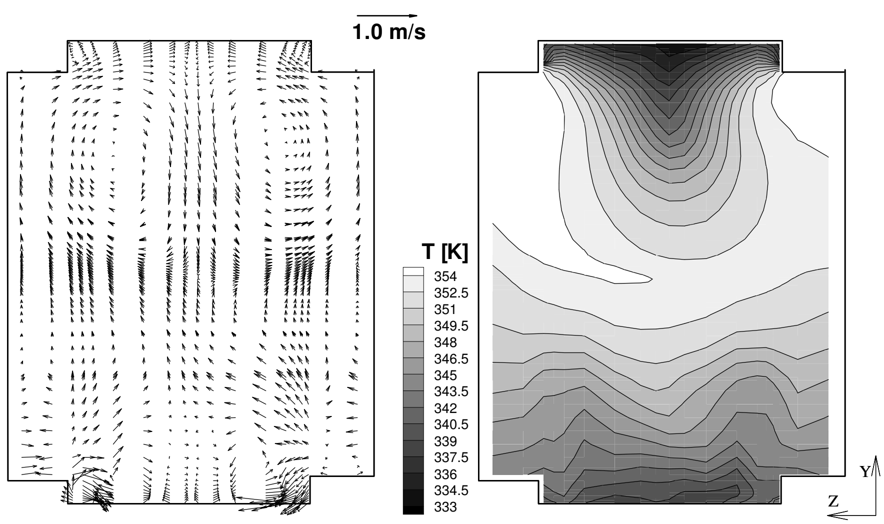

Figure 14: Steady-State Simulation Results for Wolsong 2/3/4 Moderator Using CFX-4; Side View at a Vertical Plane of x = 0.3 m

NOMENCLATURE

Ar : Archimedes number

D : tube diameter

D_e : hydraulic diameter

N_r : number of rows

L : length

P : pressure

p : pitch

Re : Reynolds number

R^{ij} : resistance tensor

u : velocity

V_m : velocity before obstruction

V_c : velocity in core region

(Greek letters)

β : thermal expansion ceofficient

γ : volume porosity

γ_A : area porosity

·e : effective viscosity

ν : kinematic viscosity

. : density

σ : standard deviation

(Subscripts)

fric : frictional

ref : reference

REFERENCES

[1] L.N. Carlucci and I. Cheung, “The Effects of Symmetric/Asymmetric Boundary Conditions on the Flow of an Internally Heated Fluid,” Numerical Methods for Partial Differential Equations, **2**, 47-61, 1986.

[2] W.M. Collins, “PHOENICS2 Model Report for Wolsong 2/3/4 Moderator Circulation Analysis,” Wolsong NPP 2/3/4, 86-03500-AR-053, Revision 0 (1995).

[3] P. Seodijono, W.M. Collins, and T. De, “Moderator Analysis for In-Core and Out-of-Core Loss of Coolant Accident (LOCA),” Wolsong NPP 2/3/4, 86-03500-AR-052, Revision 0 (1995).

[4] N.E. Todreas and M.S. Kazimi, *Nuclear System II: Elements of Thermal Hydraulic Design*, Chap. 5, Hemisphere Publishing Corporation (1990).

[5] G.I. Hadaller, R.A. Fortman, J. Szymanski, W.I. Midvidy and D.J. Train, “Fricktional Pressure Drop for Staggered and In Line Tube Bank with Large Pitch to Diameter Ratio,” Preceedings of 17th CNS Conference, Federiction, New Brunswick, Canada (1996).

[6] R.G. Huget, J.K. Szymanski, and W.I. Midvidy, “Status of Physical and Numerical Modelling of CANDU Moderator Circulation”, Proceedings of 10th Annual Conference of the Canadian Nuclear Society, Ottawa (1989).

[7] R.G. Huget, J.K. Szymanski, and W.I. Midvidy, “Experimental and Numerical Modelling of Combined Forced and Free Convection in a Complex Geometry with Internal Heat Generation”, Proceedings of 9th International Heat Transfer Conference, Vol. 3, 327 (1990).

[8] J.C. Davis, Statistics and Data Analysis in Geology, 2nd Ed., John Wiley & Sons, 1986.

[9] Churl Yoon, Bo Wook Rhee, and Byung-Joo Min, “A Study on Hydraulic Resistance of Porous Media Approach for CANDU-6 Moderator Analysis”, Proceedings of the Korean Nuclear Society Spring Meeting, Kwangju, Korea, May 2002.